

# HDAC Inhibitor-Mediated Epigenetic Regulation of Glaucoma-Associated TGF $\beta$ 2 in the Trabecular Meshwork

Jaclyn Y. Bermudez,<sup>1</sup> Hannah C. Webber,<sup>1</sup> Gaurang C. Patel,<sup>1</sup> Xiangyang Liu,<sup>2</sup> Yi-Qiang Cheng,<sup>2</sup> Abbot F. Clark,<sup>1</sup> and Weiming Mao<sup>1</sup>

<sup>1</sup>North Texas Eye Research Institute, University of North Texas Health Science Center, Fort Worth, Texas, United States

<sup>2</sup>UNT System College of Pharmacy, University of North Texas Health Science Center, Fort Worth, Texas, United States

Correspondence: Weiming Mao, North Texas Eye Research Institute, University of North Texas Health Science Center, CBH449, 3500 Camp Bowie Boulevard, Fort Worth, TX 76107, USA; Weiming.mao@unthsc.edu.

Submitted: February 26, 2016  
Accepted: June 8, 2016

Citation: Bermudez JY, Webber HC, Patel GC, et al. HDAC inhibitor-mediated epigenetic regulation of glaucoma-associated TGF $\beta$ 2 in the trabecular meshwork. *Invest Ophthalmol Vis Sci.* 2016;57:3698–3707. DOI:10.1167/iovs.16-19446

**PURPOSE.** Elevated intraocular pressure (IOP) in primary open-angle glaucoma (POAG) results from glaucomatous damage to the trabecular meshwork (TM). The glaucoma-associated factor TGF $\beta$ 2 is increased in aqueous humor and TM of POAG patients. We hypothesize that histone acetylation has a role in dysregulated TGF $\beta$ 2 expression.

**METHODS.** Protein acetylation was compared between nonglaucomatous TM (NTM) and glaucomatous TM (GTM) cells using Western immunoblotting (WB). Nonglaucomatous TM cells were treated with 10 nM thailandepsin-A (TDP-A), a potent histone deacetylase inhibitor for 4 days. Total and nuclear proteins, RNA, and nuclear protein-DNA complexes were harvested for WB, quantitative PCR (qPCR), and chromatin immunoprecipitation (ChIP) assays, respectively. Paired bovine eyes were perfused with TDP-A versus DMSO, or TDP-A versus TDP-A plus the TGF $\beta$  pathway inhibitor LY364947 for 5 to 9 days. Intraocular pressure, TM, and perfusate proteins were compared.

**RESULTS.** We found increased acetylated histone 3 and total protein acetylation in the GTM cells and TDP-A treated NTM cells. Chromatin immunoprecipitation assays showed that TDP-A induced histone hyperacetylation associated with the TGF $\beta$ 2 promoter. This change of acetylation significantly increased TGF $\beta$ 2 mRNA and protein expression in NTM cells. In perfusion-cultured bovine eyes, TDP-A increased TGF $\beta$ 2 in the perfusate as well as elevated IOP. Histologic and immunofluorescent analyses showed increased extracellular matrix and cytoskeletal proteins in the TM of TDP-A treated bovine eyes. Cotreatment with the TGF $\beta$  pathway inhibitor LY364947 blocked TDP-A-induced ocular hypertension.

**CONCLUSIONS.** Our results suggest that histone acetylation has an important role in increased expression of the glaucoma-associated factor TGF $\beta$ 2. Histone hyperacetylation may be the initiator of glaucomatous damage to the TM.

**Keywords:** glaucoma, TGF $\beta$ 2, epigenetics, trabecular meshwork, ocular hypertension

Glaucoma is a group of optic neuropathies that lead to vision loss and irreversible blindness. The most prevalent type of glaucoma is primary open-angle glaucoma (POAG). Nearly 3 million Americans are affected by this disease and over 70 million individuals are affected worldwide.<sup>1,2</sup> The number of glaucoma patients worldwide will increase to 76 million by the year 2020 and to over 111 million by 2040.<sup>2</sup> In POAG patients, elevated intraocular pressure (IOP) is the major risk factor for the development and progression of this disease.<sup>3</sup>

Intraocular pressure is regulated by the production and egress of aqueous humor (AH), a fluid that nurtures avascular anterior segment ocular tissues. Higher outflow resistance at the trabecular meshwork (TM) leads to elevated IOP in individuals with POAG. The TM is a multilayered tissue at the iridocorneal angle of the eye. The TM consists of TM cells and extracellular matrix (ECM) beams. Glaucomatous damage to the TM results in higher AH outflow resistance and, therefore, causes IOP elevation. One of the most studied pathologic changes in the glaucomatous TM (GTM) is excessive deposition of ECM material, which is believed to “clog” the TM and decrease AH outflow.

Recently, several glaucoma-associated factors have been identified. One important factor is transforming growth factor- $\beta$ 2 (TGF $\beta$ 2), an activator of the TGF $\beta$  signaling pathway. Transforming growth factor- $\beta$ 2 is a secreted protein that, when activated, binds to the TGF $\beta$  receptor type II. The binding activates TGF $\beta$  receptor type I, which phosphorylates receptor Smad proteins, Smad2/3. Phospho-Smad2/3 complexes with the co-Smad protein, Smad4, translocates into the nucleus, and regulates gene expression. TGF $\beta$ 2 also signals using non-Smad pathways, including ERK 1/2, JNK, and p38. Many studies have shown that the expression of TGF $\beta$ 2 is significantly higher in the glaucomatous AH as well as GTM tissues.<sup>4–6</sup> Activation of the TGF $\beta$  pathway by elevated TGF $\beta$ 2 leads to increased production of ECM, cytoskeletal changes, and altered cell adhesion in the TM.<sup>7–10</sup> All these TGF $\beta$ 2-induced changes in the TM also are found in the GTM,<sup>8,11,12</sup> suggesting that TGF $\beta$ 2 not only is POAG-associated, but also a causative factor of this disease. In mouse eyes as well as perfusion-cultured porcine and human eyes, overexpression of activated TGF $\beta$ 2 or treatment with recombinant TGF $\beta$ 2 elevates IOP, which leads to POAG pathology.<sup>13–16</sup>



Although TGF $\beta$ 2 and other glaucoma-associated factors have been identified and studied for years, the regulatory mechanism that causes high ocular TGF $\beta$ 2 expression is unknown. We have found that cultured GTM cells retain glaucomatous phenotypes including increased production of TGF $\beta$ 2 and ECM as well as a reorganized actin cytoskeleton.<sup>6,7,10,17</sup> Since cultured TM cells do not receive glaucomatous clues from the extracellular environment, it seems an internal mechanism is able to maintain these glaucomatous phenotypes. We believe epigenetic regulation is involved in increased production of TGF $\beta$ 2.

Epigenetic regulatory mechanisms affect gene expression without altering the genomic DNA sequence and include DNA methylation, histone modification, and RNA interference. Epigenetics has been studied extensively in development, cancers, and age-related neurodegenerative diseases, such as Alzheimer's, Parkinson's, and dementia.<sup>18-20</sup> However, the role of epigenetics in glaucoma, the leading cause of blindness worldwide, is unclear.

We previously reported that DNA methylation is not responsible for regulating another glaucoma-associated factor, sFRP1.<sup>21</sup> Gonzales et al.<sup>22</sup> reported that transfection with miR-29b mimics decreased TGF $\beta$ 2 in human TM cells at the RNA level, but had little effect on TGF $\beta$ 2 at the protein level. Therefore, we hypothesize that histone acetylation is responsible for the increased expression of TGF $\beta$ 2 in the GTM. Our strategy was to use a novel histone deacetylase inhibitor (HDACi), thailandepsin-A (TDP-A) to inhibit HDAC activities and enhance histone acetylation. This natural compound inhibits multiple classes of HDACs with high efficacy at nanomolar concentrations, which theoretically will minimize off-target effects.<sup>23</sup> We compared protein acetylation between primary nonglaucomatous human TM (NTM) and GTM cells, as well as studied the effect of altering histone acetylation on the expression of TGF $\beta$ 2 and IOP in primary NTM cell cultures and perfusion-cultured bovine eyes, respectively. Our results suggest that histone hyperacetylation may initiate glaucomatous changes in the TM. Our study is the first to show that dysregulation of histone acetylation may be one of the initiators of IOP elevation, suggesting its important role in the pathology of POAG.

## MATERIALS AND METHODS

### NTM and GTM Cell Cultures

Nonglaucomatous TM and GTM cells were characterized as described in our previous studies.<sup>6,21,24-26</sup> Briefly, TM tissues were dissected carefully from donor eyes avoiding non-TM tissue contamination and placed in culture medium on cell culture plates. After a few days, TM cells migrated from TM explants onto culture plates. All TM cells were characterized with a panel of TM markers including collagen IV, laminin,  $\alpha$ -smooth muscle actin, dexamethasone-induced myocilin expression, and formation of cross-linked actin networks. Age and sex information for these NTM and GTM cells are listed in Table 1. All HTM cells were used before senescence (less than 20 passages). Nonglaucomatous TM and GTM cells were cultured in Dulbecco's modified Eagle's low glucose medium (DMEM; Sigma-Aldrich Corp., St. Louis, MO, USA) containing 10% fetal bovine serum (FBS; Atlas Biologicals, Collins, CO, USA), 1% penicillin + streptomycin (Sigma-Aldrich Corp.), and 2 mM L-glutamine (GE Healthcare Life Sciences, Logan, UT, USA).

### Western Immunoblotting (WB)

Three primary NTM and three primary GTM cell strains were cultured to confluency. Whole cell lysates and nuclear extracts

were collected using the Mammalian Protein Extraction Reagent (M-PER; Thermo Fisher Scientific, Asheville, NC) and Nuclear and Cytoplasmic Extraction Reagent Kit (NE-PER; Thermo Fisher Scientific) according to the manufacturer's protocol, respectively. After protein estimation using the DC method (Bio-Rad, Hercules, CA, USA) or the EZQ method (Thermo Fisher Scientific, Waltham, MA, USA), proteins were separated using SDS-PAGE followed by transfer onto polyvinylidene difluoride (PVDF) membranes.

Whole cell lysate blots were probed with a rabbit polyclonal antibody against acetylated lysine residues (1:500; Cell Signaling Technology, Danvers, MA, USA) as well as a rabbit anti-GAPDH monoclonal antibody (1:1000; Cell Signaling Technology). Nuclear extract was used to detect acetylated histone 3 lysine 9/14 (Ac-H3-K9/K14) with a rabbit polyclonal antibody (1:500; Cell Signaling Technology), total histone 3 with a mouse monoclonal antibody (1:500; Abcam, Cambridge, MA, USA), and Lamin A/C with a mouse monoclonal antibody (4C11, 1:1000; Cell Signaling Technology).

Some NTM cells were cultured to confluency and were treated with 1% DMSO (Thermo Fisher Scientific) as a vehicle control or 10 nM TDP-A (purified at University of North Texas Health Science Center by Yi-Qiang Cheng and Xiangyang Liu<sup>23</sup>) for 4 days. Whole cell lysates, nuclear proteins, and conditioned medium were collected. Conditioned medium from cell cultures was concentrated with resin (StrataClean; Agilent Technologies, Santa Clara, CA, USA) at 1:100 (vol/vol). Resin was precipitated by centrifugation, and supernatant was removed. Resin was mixed with Laemmli buffer and boiled to release adsorbed proteins. Whole cell lysate, nuclear extract, and enriched conditioned medium were resolved by SDS-PAGE and transferred to PVDF membranes. The blots were probed with anti-Ac-H3-K9/K14 (1:1000), total histone 3, GAPDH, Lamin A/C, and/or TGF $\beta$ 2 (mouse monoclonal antibody, 1:500; Abcam) antibodies.

After incubation with primary antibodies, the blots were incubated with a secondary anti-rabbit or anti-mouse antibody conjugated with HRP (Cell Signaling Technology). Signals were developed using the SuperSignal West Femto Maximum Sensitivity Substrate (Thermo Fisher Scientific) or Clarity Western ECL substrate (Bio-Rad). Images were taken using the FluroChem 8900 imager (Alpha Innotech; Biomedical Solutions, Stafford, TX, USA) or the ChemiDocTM Touch imaging system (Bio-Rad). Densitometry was performed using Image J (National Institutes of Health [NIH], Bethesda, MD, USA).

### Quantitative PCR (qPCR)

Six well-characterized NTM cell strains were cultured to confluency, and treated with 1% dimethyl sulfoxide (DMSO) or 10 nM TDP-A for 4 days. RNA was extracted using an RNA purification kit (RNeasy Mini Kit; Qiagen, Valencia, CA, USA) with DNase I treatment for 15 minutes. RNA was quantified using the NanoDrop 2000 (Thermo Fisher Scientific). RNA was reverse transcribed into cDNA using the iScript cDNA synthesis kit (Bio-Rad). Quantitative PCR was performed using the SSoAdvanced SYBR Green Supermix (Bio-Rad) in a total volume of 20  $\mu$ L in a CFX96 thermocycler (Bio-Rad). The thermoprofile consisted of 40 cycles of 95°C for 10 seconds, 60°C for 30 seconds, followed by a dissociation curve. Transforming growth factor- $\beta$ 2 and GAPDH PCR primer (Sigma-Aldrich Corp.) sequences were: TGF $\beta$ 2 forward: 5'-AGATGCCTGAACAACGGATT-3',<sup>27</sup> TGF $\beta$ 2 reverse: 5'-CCATTCGCCTTCTGCTCTT-3', GAPDH forward: 5'-GGTGAAGGTCGGAGTCAAC-3',<sup>28</sup> GAPDH reverse: 5'-CCATGGGTGGAATCATATTG-3'.

TABLE 1. Cell Strain Information

Cell Strain	Age	Sex
NTM 1022-02	67	M
NTM 496-05	82	F
NTM 340-07	80	M
NTM 210-05	Unknown	F
NTM 176-04	72	M
NTM 115-01	72	Unknown
NTM 30A	Unknown	M
GTM 626-02	78	F
GTM 466-07	83	M
GTM 460-04	77	M

Data were analyzed using Wilcoxon matched-pairs signed rank test with GraphPad Prism 5 software (GraphPad, La Jolla, CA, USA).

### Chromatin Immunoprecipitation (ChIP) Assay

Three primary NTM cell strains were grown to confluency in 60-mm dishes, treated for 4 days with 1% DMSO or 10 nM TDP-A, and used for ChIP assay analysis. The SimpleChIP Enzymatic Chromatin IP Kit (Cell Signaling Technology) was used following the manufacturer's protocol. Anti-acetylated histone 3 (K9/K14) antibody (Cell Signaling Technology) was used to pull down DNA-protein complexes, and rabbit IgG was used as a control. Purified DNA was quantified by qPCR. Polymerase chain reaction primer (Sigma-Aldrich Corp.) sequences for the amplification of the TGF $\beta$ 2 promoter were: TGF $\beta$ 2 forward: 5'-GGGAGGCTGTGACTGAGCTA-3' and TGF $\beta$ 2 reverse: 5'-GTGGGTAAGGGAGGAAGGAG-3'.

The fold of enrichment method was used for data analysis.

### Bovine Anterior Segment Perfusion Organ Culture

The experimental details for this model have been described previously.<sup>24</sup> Briefly, paired bovine eyes were obtained from a local abattoir and transported to the laboratory on ice within 6 hours of sacrifice. After removal of extraocular tissues and sterilization with Betadine (Purdue Products, Stamford, CT, USA) for 2 minutes, eyes were rinsed twice with PBS. Bovine eyes were scored along the equator and the anterior segment was dissected with scissors. The vitreous, iris, uveal tract, and lens were removed carefully without disturbing the TM. The anterior segment with the cornea, sclera, and TM was mounted on a custom made Plexiglass dish. A Plexiglass O-ring was used to clamp the anterior segment at the equator to the dish using four plastic screws. This creates a watertight artificial anterior chamber. The dishes have two embedded cannulas: one allows medium infusion and the other is connected to a pressure transducer (ADI Instruments, Colorado Springs, CO, USA) to measure IOP. DMEM-high glucose medium (Thermo Fisher Scientific) containing 1% glutamine, 1% penicillin + streptomycin, and 1% amphotericin B (Sigma-Aldrich Corp.) was used as the perfusion medium. A syringe pump (PHD2000; Harvard Apparatus, Holliston, MA, USA) was used to infuse medium at a constant infusion rate of 5  $\mu$ L/min. Pressure transducers were connected to a data acquisition system (PowerLab; ADI Instruments) consisting of a signal amplifier, a bridge amplifier, and a computer with the LabChart software (ADI Instruments).

Bovine anterior segments were perfused until stable baseline IOPs were established, which usually takes approximately 24 hours. We then treated paired anterior segments for 5 to 9 days. There were two study groups: Group1 - 1%

DMSO versus 10 nM TDP-A and Group2 - 10 nM TDP-A versus 10 nM TDP-A plus 5  $\mu$ M inhibitor LY364947 (small molecule TGF $\beta$  Receptor I inhibitor; Tocris Biosciences, Ellisville, MO, USA).

Intraocular pressures were monitored and recorded every minute. Data for the 12 hours before treatment were averaged and used as baseline IOP. Intraocular pressure data after treatment were averaged every 24 hours for analysis. The change in IOP ( $\Delta$ IOP) was defined as IOP after treatment minus baseline IOP, and the highest value after treatment was defined as maximum  $\Delta$ IOP (max $\Delta$ IOP). Maximum  $\Delta$ IOP was analyzed within each group using the Student's paired *t*-test since the eyes were paired. *P* values less than 0.05 were considered statistically significant.

At the end of treatment, conditioned medium (perfusate) was collected from perfusion culture dishes and spun at 500g for 5 minutes to remove tissue debris. Equal volumes of conditioned medium were used for WB as described previously. The primary antibody used was mouse monoclonal anti TGF $\beta$ 2 antibody (1:500; Abcam).

### Histology and Immunofluorescence

Perfusion-cultured bovine anterior segments were fixed with 4% paraformaldehyde in PBS, washed three times with PBS, dehydrated with ethanol, and embedded in paraffin. Samples were sectioned at 5  $\mu$ m and stained with hematoxylin and eosin (H&E) for general evaluation or Masson's trichrome stain to study total collagen.

For immunofluorescent staining, tissue sections were deparaffinized, rehydrated, and subjected to antigen retrieval using Tris-EDTA buffer (pH 9.0) in an antigen retriever (Electron Microscopy Sciences, Hatfield, PA, USA) following manufacturer's protocol. After antigen retrieval, sections were washed with PBS, incubated with 0.5% Triton X-100 in PBS, and blocked with SuperBlock (PBS) Blocking Buffer (Thermo Fisher Scientific). Tissue sections were incubated with the anti-fibronectin rabbit polyclonal antibody (1:50; Abcam) or anti- $\alpha$ -smooth muscle actin rabbit polyclonal antibody ( $\alpha$ -SMA, 1:50; Abcam) overnight at 4°C, washed, incubated with the goat-anti-rabbit secondary antibody conjugated with Alexa-488 (1:200, Thermo Fisher Scientific), washed, and mounted with ProLong Gold Antifade Mountant containing 4',6-diamidino-2-phenylindole (DAPI; Thermo Fisher Scientific).

Images were taken using the Nikon Ti inverted microscope equipped with bright field imaging setting or long-pass filters and the Nuance Multispectral Imaging System (PerkinElmer, Waltham, MA, USA). The Nuance system uses a series of images taken at different wavelengths to create individual spectral libraries for each fluorochrome or autofluorescence (background). Based on the difference in their spectral library profiles, fluorochromes are separated from each other, and autofluorescence can be subtracted.

## RESULTS

### Protein Hyperacetylation in GTM Cells

We first compared whether there is a difference in acetylated histone 3 and total protein acetylation between NTM and GTM cells. Three NTM and three GTM cell strains were cultured to confluency, and whole cell lysate and nuclear protein were harvested for WB. We found that there was hyperacetylation in total proteins (Fig. 1A) including the lysine residues 9 and/or 14 of histone 3 (Fig. 1B) in GTM cells.

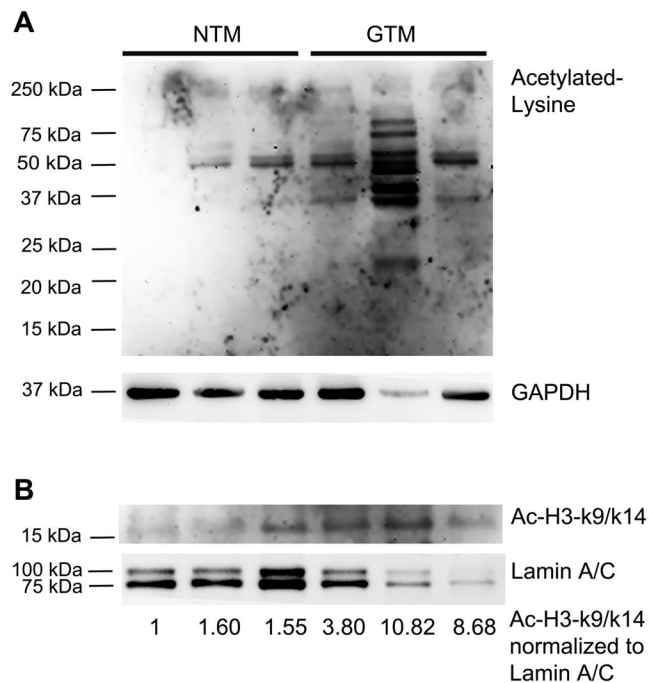


**FIGURE 1.** Increased protein acetylation in GTM cells. Western immunoblots of untreated NTM (1022-02, 340-07, 176-04) and GTM (626-02, 466-07, 460-04) cells. **(A)** Whole cell lysate was probed with an antibody against proteins with acetylated lysine residues, and GAPDH was used as a loading control. **(B)** Nuclear proteins were probed with antibodies against Ac-H3-K9/K14, and Lamin A/C was used as a nuclear protein loading control. The ratio of Ac-H3-K9/K14 to Lamin A/C was calculated using densitometry and listed at the bottom of **(B)**.

### TDP-A Increased Protein Acetylation in NTM Cell Cultures

We studied whether TDP-A was able to increase TGFβ2 expression by enhancing histone acetylation in the NTM. We tested several concentrations and found 10 nM TDP-A to be the most effective in inducing TGFβ2 expression by using qPCR (data not shown). Therefore, we treated primary NTM cells with 10 nM TDP-A or 1% DMSO as a vehicle control for 4 days. Treatment with TDP-A enhanced total protein acetylation, including histone 3 (Fig. 2), showing that TDP-A is an active HDACi for NTM cells.

### TDP-A Increased Acetylation of Histones Associated With the TGFβ2 Promoter

We performed ChIP assays to determine whether histone proteins associated with the promoter region of the TGFβ2 gene became hyperacetylated after TDP-A treatment. Histone

**TABLE 2.** ChIP Assays for Histone Acetylation Associated With the TGFβ2 Promoter

Cell Strain	DMSO	TDP-A
NTM 115-01	1.00	1.39
NTM 176-04	1.00	5.46
NTM 340-07	1.00	18.40

The anti-Ac-H3-K9/K14 antibody was used in ChIP assays to pull down DNA-protein complexes and purified DNA was quantitated by qPCR. The numbers shown represent the fold of enrichment of TGFβ2 promoter DNA.

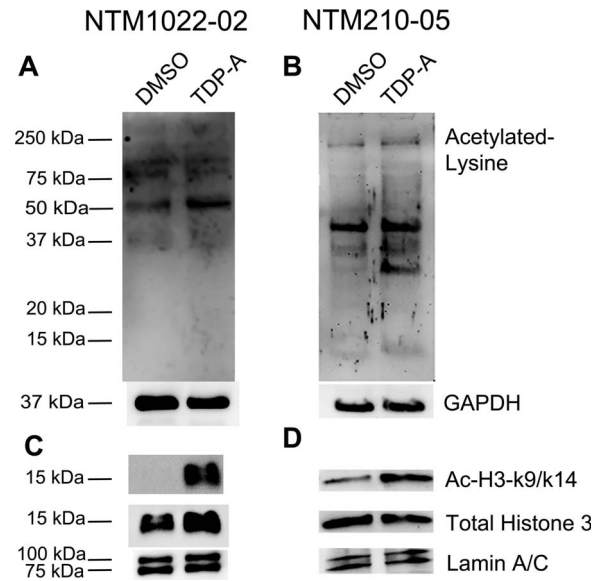


**FIGURE 2.** Histone deacetylase inhibitor TDP-A increased protein acetylation in primary NTM cells. Western immunoblots for acetylated proteins in primary TM cells treated for 4 days with DMSO or TDP-A. **(A, B)** Whole cell lysate was probed with an antibody against proteins with acetylated lysine residues, and GAPDH was used as a loading control. **(C, D)** Nuclear proteins were probed with antibodies against Ac-H3-K9/K14, total histone 3, or Lamin A/C. Lamin A/C was used as a nuclear protein loading control.

proteins have various patterns of acetylation with differential effects on transcription. Among them, Ac-H3-K9/K14 is mostly associated with the enhancement of gene expression. Therefore, we treated primary NTM cells with 10 nM TDP-A or 1% DMSO and used an anti Ac-H3-K9/K14 antibody for our ChIP assays. In all 3 NTM cell strains studied, TDP-A treatment increased acetylation of histones associated with the TGFβ2 promoter, as shown by the enrichment of TGFβ2 promoter using qPCR (Table 2).

### TDP-A Increased the Expression of TGFβ2 in NTM Cell Cultures

To determine whether histone hyperacetylation can affect the expression of the glaucoma-associated factor TGFβ2 in the TM, we treated primary NTM cells with 10 nM TDP-A or 1% DMSO as a vehicle control for 4 days. In 6 different NTM cell strains, qPCR analysis showed that TDP-A significantly elevated the expression of TGFβ2 ( $100.0 \pm 0.0\%$  vs.  $180.7 \pm 51.4\%$ , mean  $\pm$  SEM;  $P < 0.05$ ; Fig. 3A). In 3 different NTM cell strains, WB analysis showed that TDP-A elevated TGFβ2 in conditioned medium and whole cell lysates (Fig. 3B, 3C, respectively).

### TDP-A Increased IOP, TGFβ2, ECM, and Cytoskeletal Proteins in Perfusion-Cultured Bovine Eyes

Previous studies showed that elevated TGFβ2 in the TM causes ocular hypertension (OHT) in perfusion-cultured human anterior segments and in mouse eyes.<sup>13-16</sup> Since TDP-A increased the expression of TGFβ2 in TM cells, we studied whether TDP-A is able to elevate IOP as well as alter ECM and cytoskeletal proteins. We used the bovine anterior segment perfusion culture model to determine the effects of TDP-A on IOP. One of the paired bovine eyes was treated with 1% DMSO

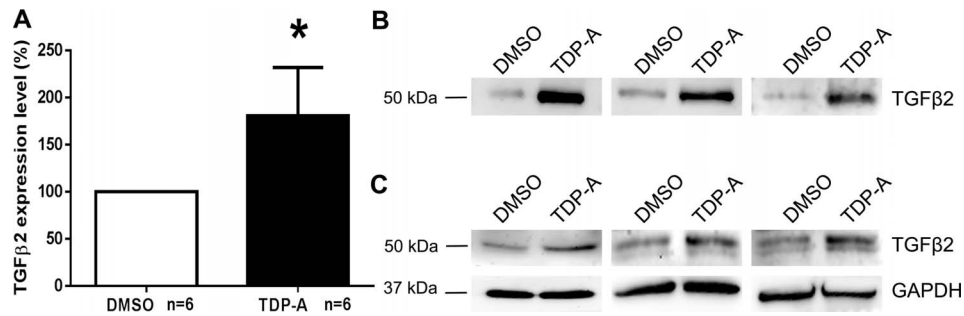


**FIGURE 3.** Thailandepsin-A increased the expression of TGFβ2 in cultured primary NTM cells. Nonglaucomatous TM cells were treated with DMSO or TDP-A for 4 days, and the expression of TGFβ2 was compared at mRNA (A) and protein (B, C) levels. (A) Quantitative PCR was used to compare the expression of TGFβ2 upon vehicle (DMSO, *open column*) or TDP-A (*shaded column*) treatment. Wilcoxon matched-pairs signed rank test was used for statistical analysis. \* $P < 0.05$ ,  $n = 6$  (NTM 1022-02, 496-05, 340-07, 210-05, 176-04, and 30A). *Columns and error bars*: means  $\pm$  SEM. (B) Conditioned medium collected from 3 different NTM cell strains (NTM 1022-02, 210-05, 176-04) was probed for TGFβ2 using WB. (C) Whole cell lysates collected from the same NTM cell strains as shown in (B) were probed for TGFβ2 using WB.

vehicle and the fellow eye was treated with 10 nM TDP-A for 5 to 9 days.

We found that TDP-A-treated eyes had significantly higher IOP compared to DMSO-treated eyes ( $\Delta$ IOP  $3.25 \pm 0.74$  vs.  $1.48 \pm 0.25$  mm Hg, mean  $\pm$  SEM;  $n = 8$ ,  $P < 0.05$ ; Figs. 4A, 4B). Western immunoblotting of perfusate (conditioned medium) also showed higher TGFβ2 protein expression in TDP-A treated eyes (Fig. 4C). To determine if DMSO or TDP-A caused any obvious morphologic changes to the bovine TM, we collected perfused bovine anterior segments for histologic studies. Light microscopic examination of H&E-stained TM tissue sections showed no apparent changes to the TM in either DMSO or TDP-A treated eyes (Figs. 4D–G). In contrast, Masson's trichrome and immunofluorescent staining showed

that TDP-A increased the expression of ECM components, including collagen and fibronectin, in the TM of perfusion-cultured bovine anterior segments (Fig. 5). Immunofluorescent staining also showed an increase in  $\alpha$ -SMA expression in the TDP-A-treated bovine TM (Fig. 6).

### The TGFβ Receptor I Inhibitor LY364947 Blocked TDP-A-Induced IOP Elevation in Perfusion-Cultured Bovine Eyes

Although TDP-A elevated IOP in perfusion-cultured bovine eyes, it is possible that this IOP elevation is mediated via other pathways or mechanisms. To rule out this possibility, we cotreated perfusion-cultured bovine eyes with TDP-A and

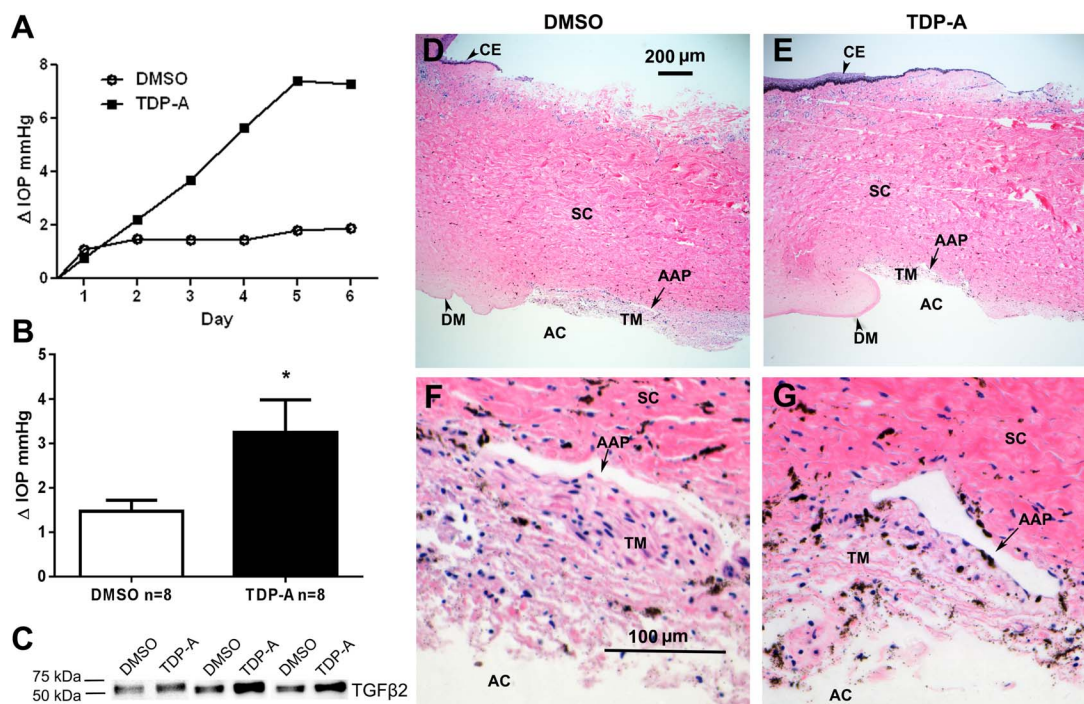


**FIGURE 4.** Thailandepsin-A increased IOP and TGFβ2 in perfusion-cultured bovine anterior segments. (A) Representative IOPs of a pair of bovine eyes perfused with or without TDP-A. (B) Mean changes in IOP after treatment with vehicle (DMSO, *open column*) or TDP-A (*shaded column*). Paired *t*-test was used for statistical analysis. \* $P < 0.05$ ;  $n = 8$ . *Columns and error bars*: means  $\pm$  SEM. (C) Perfusate (conditioned medium) collected from 3 pairs of bovine eyes was probed for TGFβ2 using WB. After 7-day perfusion culture, bovine anterior segments treated with DMSO (D, F) or TDP-A (E, G) were subjected to H&E staining to study potential morphological changes. (D, E)  $\times 40$  magnification. (F, G)  $\times 200$  magnification. AAP, angular aqueous plexus; AC, anterior chamber; CE, cornea epithelium; DM, Descemet's membrane; SC, sclera.

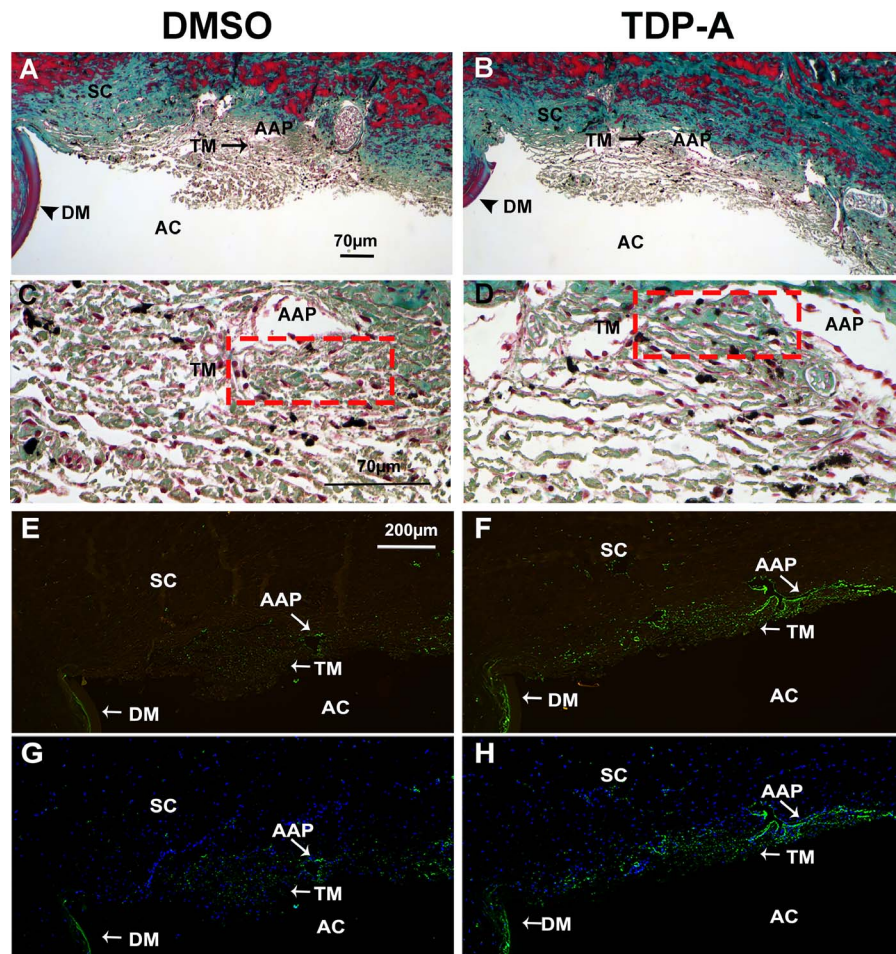


**FIGURE 5.** Thilandepsin-A increased collagen and fibronectin expression in perfusion-cultured bovine anterior segments. Perfusion-cultured bovine eyes were treated with vehicle (DMSO) or TDP-A for 7 days. At the end of perfusion, bovine anterior segments were fixed, embedded in paraffin, sectioned and used for Masson's trichrome stain for total collagen (A–D) as well as immunofluorescent staining for fibronectin (E–H). (A–D) Total collagen shown in *blue-green*. (A, B)  $\times 100$  magnification. (C, D) high magnification ( $\times 400$ ) of (A) and (B), respectively. *Red dotted boxes*: TM. (E, F) images taken using a long pass FITC filter. Fibronectin is shown in *green*, and autofluorescence is shown in *yellow-brown*, which helps to identify nonimmunostained tissues. (G, H) The same images as in (E) and (F) after autofluorescence subtraction (please see Materials and Methods for details) merged with DAPI staining (*blue*). (E–H)  $\times 100$  magnification.

LY364947, a small molecule that inhibits TGFβ signaling via preventing phosphorylation of the TGFβ receptor I. Without TGFβ receptor phosphorylation, the entire TGFβ pathway, including the Smad-dependent and -independent pathways, remain inactive. Our previous studies showed that LY364947 is a potent inhibitor that blocks both TGFβ signaling pathways in the TM.<sup>29,30</sup>

One of the paired bovine eyes was treated with TDP-A as a positive control to induce OHT, while the fellow eye was treated with TDP-A plus LY364947. The experiment was repeated in 5 pairs of bovine eyes. The eyes that were treated with TDP-A plus LY364947 showed significantly lower IOP ( $\Delta$ IOP  $2.45 \pm 0.42$  vs.  $0.78 \pm 0.36$  mm Hg, mean  $\pm$  SEM;  $n = 5$ ;  $P < 0.05$ ; Fig. 7), showing that TDP-A-induced IOP elevation is via elevated TGFβ2 expression and associated TGFβ signaling.

## DISCUSSION

In this study, we found that there is hyperacetylation at the lysine residues, especially histone 3 at lysine residues 9 and/or 14 in GTM cells compared to NTM cells. Additionally, we used in vitro and ex vivo models to demonstrate that TDP-A

induced histone hyperacetylation in the TM, which increased the expression of glaucoma-associated factor TGFβ2 as well as elevated IOP. Many studies have shown that the expression of TGFβ2 in the aqueous humor of POAG patients is elevated by approximately 50% to 100% compared to control individuals.<sup>31</sup> The same studies also showed that there is a wide range of TGFβ2 expression in nonglaucomatous individuals, which may explain the variation in histone acetylation seen in our ChIP data (Table 2). Furthermore, the IOP elevation we observed was TGFβ2-dependent because it could be blocked by a TGFβ receptor inhibitor. In the tissue of perfusion-cultured anterior segments, we found that TDP-A increased total collagen, fibronectin, and  $\alpha$ -SMA expression. In the TM, these changes have been reported previously to be TGFβ2 inducible,<sup>7,12,32</sup> further suggesting that our findings were very likely to be caused by TDP-A-induced TGFβ2 elevation in bovine eyes. The HDAC inhibitor TDP-A-induced IOP elevation was 3.25 mm Hg, which was statistically significant in the bovine anterior segment perfusion culture model. In our previous studies using the same model to investigate glucocorticoid-induced glaucoma, we found dexamethasone elevated IOP by more than 2.82 mm Hg.<sup>24</sup> In this study, TDP-A elevated IOP by more than 3 mm Hg, which is statistically and

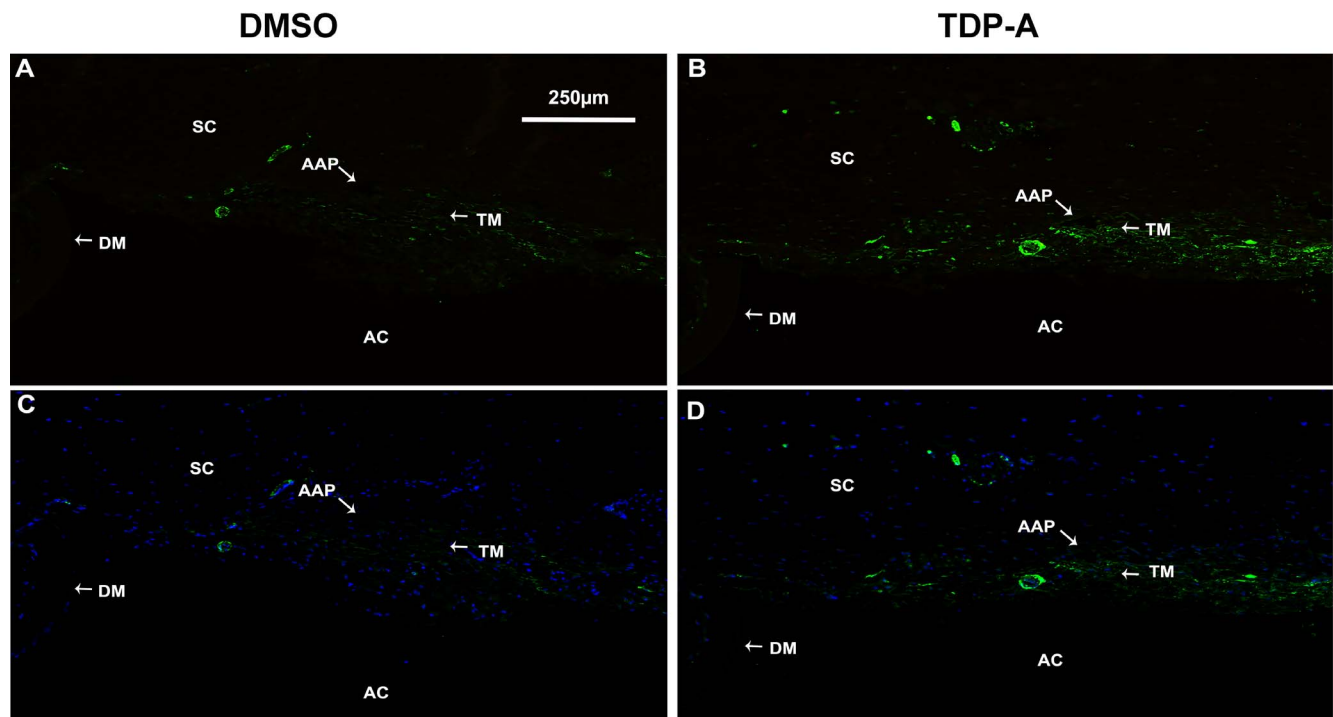


**FIGURE 6.** Thilandepsin-A increased  $\alpha$ -SMA in perfusion-cultured bovine anterior segments. Perfusion-cultured bovine eyes were treated with vehicle (DMSO) or TDP-A for 7 days. At the end of perfusion, bovine anterior segments were fixed, embedded in paraffin, sectioned, and stained for  $\alpha$ -SMA (green). Nuclei were stained with DAPI (blue). Magnification:  $\times 100$ . (A, B) images were taken using a long pass FITC filter. Autofluorescence is shown in yellow-brown, which helps to identify nonimmunostained tissues. (C, D) the same images as in (A) and (B) after autofluorescence subtraction (please see Materials and Methods for details) merged with DAPI staining (blue).

functionally significant. Taken together, our results showed that histone hyperacetylation may have an important role in the increased expression of glaucoma-associated factor TGFβ2. To our knowledge, this is the first report showing

that abnormal histone acetylation may initiate the glaucoma pathologic changes to the TM.

Epigenetic regulation has been shown to have vital roles in a number of diseases. DNA methylation is associated with gene suppression. In cancers, DNA hypermethylation decreases the expression of tumor suppressor genes, which leads to tumorigenesis.<sup>33</sup> In Alzheimer's disease, changes in global and/or gene-specific DNA methylation have been reported.<sup>34</sup> However, in POAG, we found that DNA methylation is not the regulatory mechanism responsible for the increased expression of the glaucoma-associated factor sFRP1 in the TM.<sup>21,35</sup> MicroRNA regulation also contributes to cancers and neurodegenerative diseases. Different from artificial siRNA, miRNA silences a number of genes. Differential expression of different miRNAs, such as miR-15, -16 and miR-21, -155 have been found to suppress or promote tumors, respectively.<sup>36</sup> In the eye, Gonzalez et al.<sup>37</sup> showed that miR-200c may have a role in TM cell contraction and IOP regulation.

In contrast to DNA methylation and miRNA, which inhibit gene expression, histone acetylation generally increases gene expression. This modification unwinds chromatin, facilitates transcription factor and cofactor binding, and enhances gene transcription. The balance of histone acetylation is maintained by HDACs and histone acetyl transferases (HATs). In chronic obstructive pulmonary diseases, a profound loss of HDAC2 has been reported, which may mediate the upregulation of inflammatory genes and lower responses to steroids.<sup>38</sup> In Parkinson's disease, hyperacetylation of H3 or H4 are the key findings in dopaminergic neurons, which may promote neuronal apoptosis.<sup>20</sup> Nickels et al.<sup>39,40</sup> showed that HDAC3 and 4 participate in retinal ganglion cell apoptosis in experimental models of glaucoma.

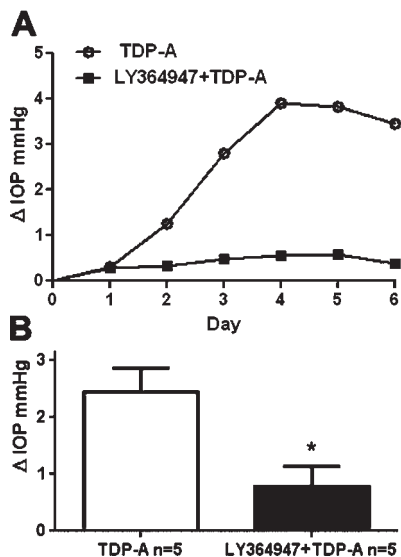


**FIGURE 7.** The TGFβ receptor I inhibitor LY364947 prevented TDP-A induced IOP elevation. (A) Representative IOPs of a pair of bovine eyes treated with TDP-A ± TGFβ signaling inhibitor LY364947. (B) The IOP of perfusion-cultured bovine eyes treated with TDP-A alone (open column) or TDP-A + LY364947 (shaded column). Paired *t*-test was used for statistical analysis. \**P* < 0.05; *n* = 5. Columns and error bars: means ± SEM.

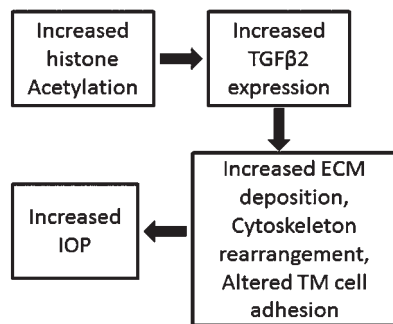


FIGURE 8. Schematic of histone acetylation in IOP regulation.

Although HDACs can have positive or negative roles in diseases, most studies showed that HDAC inhibitors are protective, especially in neural diseases. The mechanism by which HDAC inhibitors protect cells or neurons still is not fully understood. They may enhance the expression of molecules, such as neurotrophins and their receptors, Bcl-2, AKT, and nestin that promote neuronal survival, inhibit apoptosis, or induce neural regeneration.<sup>41</sup> Under experimental glaucomatous conditions, valproic acid (another HDACi) has been shown to protect RGCs in rat ischemia/reperfusion and ocular hypertension models.<sup>42,43</sup> In DBA/2J mice, a pigmented glaucoma model that develops ocular hypertension, trichostatin (another HDACi) improves the expression of a subset of RGC genes that are downregulated during this disease process.<sup>44</sup> Since HDAC inhibitors change global gene expression, beneficial and detrimental genes may be affected. However, it is possible that the promoters of the genes that are involved in disease pathways are hypoacetylated compared to other genes. Therefore, these disease-associated genes are more likely to be rescued by HDACi treatment, while the expression of other disease-irrelevant genes may not change. This may explain why HDAC inhibitors have various therapeutic effects, such as enhancement of cell survival as well as inhibition of tumor growth. In contrast, we found that HDAC inhibitors may adversely upregulate the expression of glaucoma-associated factors such as TGFβ2, leading to elevated IOP. In the TM, HDAC-induced expression of TGFβ2 appeared responsible for the TDP-A-induced OHT. Therefore, the overall effect of HDAC inhibitors is very likely to be tissue- and disease-dependent and should be determined on a case-by-case basis. Also, how TDP-A affects GTM cells may be different from our NTM data, which needs further investigation.

Histone deacetylase inhibitors have five classes and multiple isomers. They not only modify histones, but also bind to and/or modify other transcription factors.<sup>20</sup> It will be very interesting to find out which HDAC(s) is specific for the regulation of TGFβ2 as well as other glaucoma-associated factors in the TM. Additionally, similar to glaucomatous TM cells, glaucomatous lamina cribrosa (LC) cells, a specialized cell type in the optic nerve head (ONH) that is a primary site of glaucomatous optic neuropathy, have been shown to have increased expression of TGFβ2.<sup>26,45</sup> Glaucomatous LC cells also demonstrate increased ECM deposition and cytoskeletal changes that can be induced by TGFβ2 just like TM cells.<sup>26,46,47</sup> Thus, it is possible that histone hyperacetylation also is responsible for the increased expression of TGFβ2 in the glaucomatous ONH.

Since we found that an HDACi elevated IOP, it is reasonable to speculate that histone acetyl transferase inhibitors would decrease TGFβ2 expression and lower IOP. Histone acetyl transferases are enzymes that increase histone acetylation. Similar to HDACs, they also can bind to other transcription factors and regulate gene expression. Histone acetyl transfer-

ases generally function as transcriptional coactivators. The 17 human HATs are divided into five classes.<sup>48</sup> In contrast to the diversity of various HDAC inhibitors, not many HAT inhibitors are available. Several HAT inhibitors, such as anacardic acid and curcumin, have been shown to inhibit Jurkat T-cell leukemia cells and prevent heart failure in rats, respectively.<sup>49,50</sup> Kanthasamy et al.<sup>51</sup> showed that anacardic acid attenuated dieldrin-induced damage in primary mesencephalic cells.<sup>51</sup> Like HDAC inhibitors, HAT inhibitors may affect genes that are selectively activated in POAG. Thus, HAT inhibitors may be a potential therapeutic approach in treating POAG.

We have provided evidence supporting the role of epigenetic regulation of TGFβ2 as a glaucoma mediator that elevates IOP. However, other glaucoma-associated factors such as sFRP1,<sup>52</sup> gremlin,<sup>7</sup> serum amyloid A,<sup>52</sup> sCD44,<sup>53</sup> and cochlin,<sup>54</sup> also may be epigenetically regulated to elevate IOP. Although these factors have been elevated in POAG AH and/or TM, to our knowledge, there have not been any studies to find out whether some or all of them are coexpressed in POAG patients. If that is true, it is very likely that the other glaucoma-associated factors are elevated in POAG via a similar epigenetic mechanism as TGFβ2.

In summary, our findings suggested epigenetic regulation as a novel mechanism in TM pathogenesis and IOP regulation (Fig. 8). Further research is needed to help better understand the role of epigenetics in POAG. Our discovery may provide novel therapeutic strategies and targets for treating glaucoma.

### Acknowledgments

The authors thank Sandra Maansson for assistance in histology.

Supported by the Thomas R. Lee award for National Glaucoma Research (G2011032), a program of the Bright Focus Foundation (WM), National Eye Institute R21EY023048 (WM), UNTHSC faculty seed grant (WM), a research grant provided by Cure Glaucoma Foundation (WM), National Cancer Institute CA152212 (Y-QC), and NIH training grant in the Neurobiology of Aging (T32 AG20494; JYB).

Disclosure: **J.Y. Bermudez**, None; **H.C. Webber**, None; **G.C. Patel**, None; **X. Liu**, None; **Y.-Q. Cheng**, None; **A.F. Clark**, None; **W. Mao**, None

### References

- Congdon N, O'Colmain B, Klaver CC, et al. Causes and prevalence of visual impairment among adults in the United States. *Arch Ophthalmol*. 2004;122:477-485.
- Tham YC, Li X, Wong TY, Quigley HA, Aung T, Cheng CY. Global prevalence of glaucoma and projections of glaucoma burden through 2040: a systematic review and meta-analysis. *Ophthalmology*. 2014;121:2081-2090.
- The Advanced Glaucoma Intervention Study (AGIS): 7. The relationship between control of intraocular pressure and visual field deterioration. The AGIS Investigators. *Am J Ophthalmol*. 2000;130:429-440.
- Tripathi RC, Li J, Chan WF, Tripathi BJ. Aqueous humor in glaucomatous eyes contains an increased level of TGF-beta 2. *Exp Eye Res*. 1994;59:723-727.
- Inatani M, Tanihara H, Katsuta H, Honjo M, Kido N, Honda Y. Transforming growth factor-beta 2 levels in aqueous humor of glaucomatous eyes. *Graefes Arch Clin Exp Ophthalmol*. 2001; 239:109-113.
- Tovar-Vidales T, Clark AF, Wordinger RJ. Transforming growth factor-beta2 utilizes the canonical Smad-signaling pathway to regulate tissue transglutaminase expression in human trabecular meshwork cells. *Exp Eye Res*. 2011;93:442-451.
- Wordinger RJ, Fleenor DL, Hellberg PE, et al. Effects of TGF-beta2, BMP-4, and gremlin in the trabecular meshwork:



- implications for glaucoma. *Invest Ophthalmol Vis Sci.* 2007; 48:1191-1200.
8. Wecker T, Han H, Borner J, Grehn F, Schlunck G. Effects of TGF-beta2 on cadherins and beta-catenin in human trabecular meshwork cells. *Invest Ophthalmol Vis Sci.* 2013;54:6456-6462.
  9. O'Reilly S, Pollock N, Currie L, Paraoan L, Clark AF, Grierson I. Inducers of cross-linked actin networks in trabecular meshwork cells. *Invest Ophthalmol Vis Sci.* 2011;52:7316-7324.
  10. Clark AF, Miggans ST, Wilson K, Browder S, McCartney MD. Cytoskeletal changes in cultured human glaucoma trabecular meshwork cells. *J Glaucoma.* 1995;4:183-188.
  11. Hoare MJ, Grierson I, Brochie D, Pollock N, Cracknell K, Clark AF. Cross-linked actin networks (CLANs) in the trabecular meshwork of the normal and glaucomatous human eye in situ. *Invest Ophthalmol Vis Sci.* 2009;50:1255-1263.
  12. Wordinger RJ, Sharma T, Clark AF. The role of TGF-beta2 and bone morphogenetic proteins in the trabecular meshwork and glaucoma. *J Ocul Pharmacol Ther.* 2014;30:154-162.
  13. Shepard AR, Millar JC, Pang IH, Jacobson N, Wang WH, Clark AF. Adenoviral gene transfer of active human transforming growth factor-(beta)2 elevates intraocular pressure and reduces outflow facility in rodent eyes. *Invest Ophthalmol Vis Sci.* 2010;51:2067-2076.
  14. Fleenor DL, Shepard AR, Hellberg PE, Jacobson N, Pang IH, Clark AF. TGFbeta2-induced changes in human trabecular meshwork: implications for intraocular pressure. *Invest Ophthalmol Vis Sci.* 2006;47:226-234.
  15. Gottanka J, Chan D, Eichhorn M, Lutjen-Drecoll E, Ethier CR. Effects of TGF-beta2 in perfused human eyes. *Invest Ophthalmol Vis Sci.* 2004;45:153-158.
  16. McDowell CM, Tebow HE, Wordinger RJ, Clark AF. Smad3 is necessary for transforming growth factor-beta2 induced ocular hypertension in mice. *Exp Eye Res.* 2013;116:419-423.
  17. Wallace DM, Murphy-Ullrich JE, Downs JC, O'Brien CJ. The role of matricellular proteins in glaucoma. *Matrix Biol.* 2014; 37:174-182.
  18. Daniel M, Tollefsbol TO. Epigenetic linkage of aging, cancer and nutrition. *J Exp Biol.* 2015;218:59-70.
  19. Traynor BJ, Renton AE. Exploring the epigenetics of Alzheimer disease. *JAMA Neurol.* 2015;72:8-9.
  20. Feng Y, Jankovic J, Wu YC. Epigenetic mechanisms in Parkinson's disease. *J Neurol Sci.* 2015;349:3-9.
  21. Mao W, Rubin JS, Anoruo N, Wordinger RJ, Clark AF. SFRP1 promoter methylation and expression in human trabecular meshwork cells. *Exp Eye Res.* 2012;97:130-136.
  22. Luna C, Li G, Qiu J, Epstein DL, Gonzalez P. Cross-talk between miR-29 and transforming growth factor-betas in trabecular meshwork cells. *Invest Ophthalmol Vis Sci.* 2011;52:3567-3572.
  23. Wang C, Henkes LM, Doughty LB, et al. Thailandepsins: bacterial products with potent histone deacetylase inhibitory activities and broad-spectrum antiproliferative activities. *J Nat Prod.* 2011;74:2031-2038.
  24. Mao W, Tovar-Vidales T, Yorio T, Wordinger RJ, Clark AF. Perfusion-cultured bovine anterior segments as an ex vivo model for studying glucocorticoid-induced ocular hypertension and glaucoma. *Invest Ophthalmol Vis Sci.* 2011;52:8068-8075.
  25. Wordinger RJ, Clark AF, Agarwal R, et al. Cultured human trabecular meshwork cells express functional growth factor receptors. *Invest Ophthalmol Vis Sci.* 1998;39:1575-1589.
  26. Zode GS, Sethi A, Brun-Zinkernagel AM, Chang IF, Clark AF, Wordinger RJ. Transforming growth factor-beta2 increases extracellular matrix proteins in optic nerve head cells via activation of the Smad signaling pathway. *Mol Vis.* 2011;17: 1745-1758.
  27. Pavan L, Tarrade A, Hermouet A, et al. Human invasive trophoblasts transformed with simian virus 40 provide a new tool to study the role of PPARgamma in cell invasion process. *Carcinogenesis.* 2003;24:1325-1336.
  28. Martens JW, Sieuwerts AM, Bolt-deVries J, et al. Aging of stromal-derived human breast fibroblasts might contribute to breast cancer progression. *Thromb Haemost.* 2003;89:393-404.
  29. Sethi A, Jain A, Zode GS, Wordinger RJ, Clark AF. Role of TGFbeta/Smad signaling in gremlin induction of human trabecular meshwork extracellular matrix proteins. *Invest Ophthalmol Vis Sci.* 2011;52:5251-5259.
  30. Sethi A, Mao W, Wordinger RJ, Clark AF. Transforming growth factor-beta induces extracellular matrix protein cross-linking lysyl oxidase (LOX) genes in human trabecular meshwork cells. *Invest Ophthalmol Vis Sci.* 2011;52:5240-5250.
  31. Agarwal P, Daher AM, Agarwal R. Aqueous humor TGF-beta2 levels in patients with open-angle glaucoma: a meta-analysis. *Mol Vis.* 2015;21:612-620.
  32. Pattabiraman PP, Rao PV. Mechanistic basis of Rho GTPase-induced extracellular matrix synthesis in trabecular meshwork cells. *Am J Physiol Cell Physiol.* 2010;298:C749-C763.
  33. Fukui T, Kondo M, Ito G, et al. Transcriptional silencing of secreted frizzled related protein 1 (SFRP 1) by promoter hypermethylation in non-small-cell lung cancer. *Oncogene.* 2005;24:6323-6327.
  34. Lu H, Liu X, Deng Y, Qing H. DNA methylation, a hand behind neurodegenerative diseases. *Front Aging Neurosci.* 2013;5:85.
  35. Wang WH, McNatt LG, Pang IH, et al. Increased expression of the WNT antagonist sFRP-1 in glaucoma elevates intraocular pressure. *J Clin Invest.* 2008;118:1056-1064.
  36. Li Y, Kowdley KV. MicroRNAs in common human diseases. *Genom Proteom Bioinform.* 2012;10:246-253.
  37. Luna C, Li G, Huang J, et al. Regulation of trabecular meshwork cell contraction and intraocular pressure by miR-200c. *PLoS One.* 2012;7:e51688.
  38. Barnes PJ, Adcock IM, Ito K. Histone acetylation and deacetylation: importance in inflammatory lung diseases. *Eur Respir J.* 2005;25:552-563.
  39. Schmitt HM, Pelzel HR, Schlamp CL, Nickells RW. Histone deacetylase 3 (HDAC3) plays an important role in retinal ganglion cell death after acute optic nerve injury. *Mol Neurodegener.* 2014;9:39.
  40. Pelzel HR, Schlamp CL, Nickells RW. Histone H4 deacetylation plays a critical role in early gene silencing during neuronal apoptosis. *BMC Neurosci.* 2010;11:62.
  41. Lu J, Frerich JM, Turtzo LC, et al. Histone deacetylase inhibitors are neuroprotective and preserve NGF-mediated cell survival following traumatic brain injury. *Proc Natl Acad Sci U S A.* 2013;110:10747-10752.
  42. Zhang Z, Qin X, Zhao X, et al. Valproic acid regulates antioxidant enzymes and prevents ischemia/reperfusion injury in the rat retina. *Curr Eye Res.* 2012;37:429-437.
  43. Alsarraf O, Fan J, Dahrouj M, Chou CJ, Yates PW, Crosson CE. Acetylation preserves retinal ganglion cell structure and function in a chronic model of ocular hypertension. *Invest Ophthalmol Vis Sci.* 2014;55:7486-7493.
  44. Pelzel HR, Schlamp CL, Waclawski M, Shaw MK, Nickells RW. Silencing of Fem1cR3 gene expression in the DBA/2J mouse precedes retinal ganglion cell death and is associated with histone deacetylase activity. *Invest Ophthalmol Vis Sci.* 2012; 53:1428-1435.
  45. Pena JD, Taylor AW, Ricard CS, Vidal I, Hernandez MR. Transforming growth factor beta isoforms in human optic nerve heads. *Br J Ophthalmol.* 1999;83:209-218.
  46. Fuchshofer R, Birke M, Welge-Lussen U, Kook D, Lutjen-Drecoll E. Transforming growth factor-beta 2 modulated

- extracellular matrix component expression in cultured human optic nerve head astrocytes. *Invest Ophthalmol Vis Sci.* 2005; 46:568-578.
47. Job R, Raja V, Grierson I, et al. Cross-linked actin networks (CLANs) are present in lamina cribrosa cells. *Br J Ophthalmol.* 2010;94:1388-1392.
  48. Haery L, Thompson RC, Gilmore TD. Histone acetyltransferases and histone deacetylases in B- and T-cell development, physiology and malignancy. *Genes Cancer.* 2015;6:184-213.
  49. Eliseeva ED, Valkov V, Jung M, Jung MO. Characterization of novel inhibitors of histone acetyltransferases. *Mol Cancer Ther.* 2007;6:2391-2398.
  50. Morimoto T, Sunagawa Y, Kawamura T, et al. The dietary compound curcumin inhibits p300 histone acetyltransferase activity and prevents heart failure in rats. *J Clin Invest.* 2008; 118:868-878.
  51. Song C, Kanthasamy A, Anantharam V, Sun F, Kanthasamy AG. Environmental neurotoxic pesticide increases histone acetylation to promote apoptosis in dopaminergic neuronal cells: relevance to epigenetic mechanisms of neurodegeneration. *Mol Pharmacol.* 2010;77:621-632.
  52. Wang WH, McNatt LG, Pang IH, et al. Increased expression of serum amyloid A in glaucoma and its effect on intraocular pressure. *Invest Ophthalmol Vis Sci.* 2008;49:1916-1923.
  53. Knepper PA, Goossens W, Mayanil CS. CD44H localization in primary open-angle glaucoma. *Invest Ophthalmol Vis Sci.* 1998;39:673-680.
  54. Bhattacharya SK, Rockwood EJ, Smith SD, et al. Proteomics reveal Cochlin deposits associated with glaucomatous trabecular meshwork. *J Biol Chem.* 2005;280:6080-6084.